# Anchoring Energy Acceptors to Nanostructured ZrO2 Enhances Photon Upconversion by Sensitized Triplet−Triplet Annihilation Under Simulated Solar Flux

**ARTICLE** *in* THE JOURNAL OF PHYSICAL CHEMISTRY C · JULY 2013

Impact Factor: 4.77 · DOI: 10.1021/jp402477q



**6 AUTHORS**, INCLUDING:

Djawed Nauroozi
Universität Ulm
**10** PUBLICATIONS **41** CITATIONS

SEE PROFILE

Marie-Pierre Santoni
Paris Diderot University
**30** PUBLICATIONS **272** CITATIONS

SEE PROFILE

THE JOURNAL OF PHYSICAL CHEMISTRY C

Article

pubs.acs.org/JPCC

# Anchoring Energy Acceptors to Nanostructured $ZrO_2$ Enhances Photon Upconversion by Sensitized Triplet−Triplet Annihilation Under Simulated Solar Flux

Jonas Sandby Lissau,[†] Djawed Nauroozi,[†] Marie-Pierre Santoni,[†] Sascha Ott,[†] James M. Gardner,[‡] and Ana Morandeira*[,†]

[†]Department of Chemistry - Ångström Laboratory, Uppsala University, Box 523, SE-75120 Uppsala, Sweden

[‡]Department of Chemistry - Division of Applied Physical Chemistry, KTH Royal Institute of Technology, SE-10044 Stockholm, Sweden

Supporting Information

**ABSTRACT:** Photon upconversion by sensitized triplet−triplet annihilation (UC-STTA) is a promising strategy for boosting the theoretical maximum efficiency of single threshold solar cells, in particular, dye-sensitized solar cells (DSSCs). Here, we report a substantial increase in the efficiency of UC-STTA on a nanostructured surface, using noncoherent excitation light with intensities as low as 0.5 mW $cm^{-2}$, easily achieved under sun illumination. The studied surface was a mesoporous $ZrO_2$ film working as a proxy system for the study of photophysics relevant to DSSCs. A well-known UC-STTA "emitter" dye, 9,10-diphenylanthracene (DPA), was chemically modified to yield methyl 4-(10-*p*-tolylanthracen-9-yl)benzoate (MTAB), which was chemisorbed onto $ZrO_2$. The "sensitizer" dye, platinum(II) octaethylporphyrin (PtOEP), was free in butyronitrile (BuN) solution surrounding the $ZrO_2$ nanostructure. A rigorous oxygen removal minimized photodegradation of the dyes and enhanced triplet−triplet annihilation efficiency. The system already approaches the so-called "strong annihilation limit" at light intensities below 8 mW $cm^{-2}$. Highly efficient triplet−triplet annihilation is a requisite for the use of UC-STTA in DSSCs. Time-resolved data show that the limiting process in the UC-STTA mechanism of the present system is the dynamic triplet energy transfer step from PtOEP in solution to MTAB on the surface of $ZrO_2$. This result can guide the way toward a better understanding and further efficiency improvement of UC-STTA on nanocrystalline metal oxides.

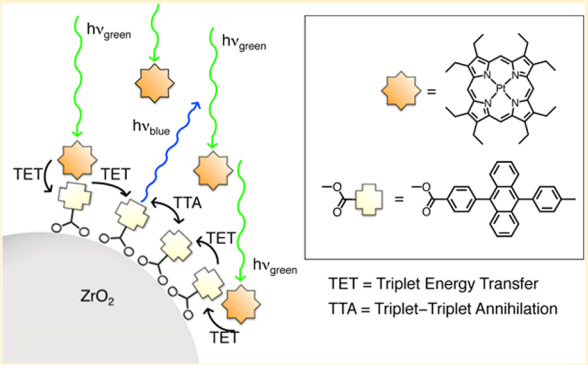


## INTRODUCTION

Photon upconversion (UC) is the conversion of two or more photons of low energy into a single photon of higher energy. There exist several different mechanisms for UC; the most well-known mechanisms rely on nonlinear optical crystals and high-intensity coherent laser radiation.[1] In recent years attention has been given to alternative mechanisms for upconversion that can occur in the absence of expensive rare-earth optical crystals and under low-intensity noncoherent light. Upconversion may therefore have potential for applications in solar cells. Implementation of the UC principle in solar cells opens a way to overcome the Shockley−Queisser limit for solar energy conversion efficiency that is common to all single-threshold solar cells.[2] A number of studies have been carried out to explore the potential of using UC schemes based on rare-earth metal ions in solar cells (references 3 and 4 provide reviews). Recently, a mixed UC scheme using organic dyes for the sensitization of rare-earth metal ions was investigated.[5]

An alternative route to UC is via sensitized triplet−triplet annihilation (UC-STTA). In the UC-STTA mechanism, a "sensitizer" molecule (S) with a high singlet-to-triplet intersystem-crossing (ISC) yield absorbs a low-energy photon

$$S + h\nu_{low} \rightarrow {}^1S^* \quad (1)$$

The resulting singlet excited state relaxes to a triplet excited state

$${}^1S^* \rightarrow {}^3S^* \quad (2)$$

The triplet excited state of the "sensitizer" is then transferred to an "emitter" molecule (E), by triplet energy transfer (TET), producing an "emitter" triplet

$${}^3S^* + E \rightarrow S + {}^3E^* \quad (3)$$

When two triplet "emitter" molecules encounter each other, triplet−triplet annihilation (TTA) may occur. The TTA process can result in production of a singlet excited state for

**Received:** March 11, 2013
**Revised:** June 10, 2013
**Published:** July 3, 2013

   dx.doi.org/10.1021/jp402477q | J. Phys. Chem. C 2013, 117, 14493−14501

the "emitter" molecule that is higher in energy than the initial singlet excited state for the "sensitizer"

$$^3E^* + {}^3E^* \rightarrow E + {}^1E^* \quad (4)$$

In the absence of quenching mechanisms, such as electron transfer or nonradiative decay, this type of UC can be observed as delayed anti-Stokes fluorescence from the "emitter" singlet excited state

$$^1E^* \rightarrow E + h\nu_{high} \quad (5)$$

UC-STTA can occur under sunlight-like conditions due to the long-lived molecular triplet excited states working as intermediate energy levels in the UC process.[6] The mechanism also benefits from the large absorption cross sections of the dye molecules involved in this UC strategy as compared to rare-earth metal ions,[3,7] as well as the option to tune the energy levels involved to a desired spectral region. The past decade has seen a renewed interest in UC-STTA systems,[8−11] pioneered by Baluschev[12] and Castellano.[13] Early studies mainly focused on UC-STTA in solution since UC-STTA in solid-state materials was, by comparison, very inefficient. However, in the last couple of years there have been dramatic improvements on the efficiency of solid-state systems. At the moment, the most UC-STTA efficient solid-state systems are those where the sensitizer and emitter dyes are embedded in rubbery polymer matrixes.[14,15] These matrixes allow a certain degree of dye mobility at room temperature and have the additional advantage of inhibiting quenching by oxygen and leading to UC efficiencies exceeding 20% at a moderate excitation power density of ∼100 mW/cm$^2$.[16] The UC-STTA principle has recently been explored for increasing the solar energy conversion efficiency in hydrogenated amorphous silicon and organic bulk heterojunction solar cells[17,18] and as a sub-bandgap sensitizing process for a photoelectrochemical reaction[19] and for semiconductor photocatalysis.[20] There is also a growing interest in the development of upconverting nanocapsules,[21] particularly in the field of bioimaging.[22]

Ekins-Daukes and Schmidt have shown that implementation of UC-STTA in dye-sensitized solar cells (DSSCs) would raise the theoretical efficiency limit of these devices from ∼30% to more than 40%.[23] Such implementation would require adsorption of the emitter dye to the surface of a photoactive electrode. This approach is very different from the above-mentioned rubbery polymer matrixes or nanocapsules. In the case of sensitized nanostructured metal oxides, molecular diffusion of the adsorbed dye will be greatly reduced, and energy migration between neighboring molecules will play a key role in the efficiency of the TTA process. Recently, we reported the first proof-of-principle results for this concept by showing that UC-STTA is possible on a dye-sensitized nanostructured metal oxide under sunlight-like conditions.[24] In this proof-of-principle system, the platinum(II) octaethylporphyrin (PtOEP)/9,10-diphenylanthracene (DPA) sensitizer/emitter pair was physisorbed onto a mesoporous $ZrO_2$ film and subsequently immersed into water purged with argon. To determine if we could generate UC-STTA and observe the singlet excited state of DPA, we opted to work on $ZrO_2$ because the high energy of the conduction band[25] inhibits electron injection from excited dyes adsorbed onto the nanostructure and allows for the observation of anti-Stokes emission from the DPA singlet excited state. The structural properties and refractive index of mesoporous $ZrO_2$ are very similar to mesoporous $TiO_2$,[26] which is the semiconductor used in DSSCs. In these regards, $ZrO_2$ is a good proxy system for studying photophysical properties of dyes in DSSCs.[25,26] By exciting the described system at the Q-band of PtOEP using low intensity noncoherent light (8 mW/cm$^2$), we were able to detect anti-Stokes emission from the singlet excited state of DPA, thus confirming the UC-STTA process.[24] A fast rise of the UC signal indicated that the UC-STTA proceeded via Dexter-type energy migration through dye molecules adsorbed onto the surface of $ZrO_2$.

While the initial test system described above was successful in showing the feasibility of UC-STTA on a nanostructured metal oxide under sunlight-like conditions, it is probable that the efficiency of the process was greatly limited by a set of unfavorable inherent properties of the system.[24] A potential limitation of this system was that a fraction of the adsorbed PtOEP molecules formed aggregates, which might trap excitation energy and thereby decrease the efficiency of UC-STTA. Also, the molecules used did not contain anchor groups, resulting in nonoptimal dye loading on the metal oxide surface. We anticipated that the nonpolar DPA molecules would lay flat on the surface due to the polar aqueous environment surrounding the nanostructure. The UC-STTA mechanism involves Dexter-type energy transfer, which requires orbital overlap between the involved molecules, and with an insufficient dye loading a poor orbital overlap is expected to limit the overall UC-STTA efficiency. Also, the electrostatics of the system, polar solvent and nonpolar DPA, was thought to decrease further the orbital overlap between adsorbed dyes because these would be in unfavorable orientations (laying flat on the surface) for energy transfer.

Finally, due to the central role that triplet excited states play in the UC-STTA scheme, the mechanism is extremely sensitive to the presence of oxygen, which is an efficient quencher of triplets. The oxygen concentration was decreased by bubbling argon into the cuvette containing the studied system. This method is known to be nonoptimal for oxygen removal in mesoporous systems due to inherently low diffusion rates. We had clear indications that the singlet oxygen produced in the quenching process caused dye degradation and thereby added further restriction upon the UC efficiency.[24]

For the system studied in this paper (depicted in Chart 1), we aim to address the issues described above, to improve the efficiency of UC-STTA on mesoporous surfaces. For this reason, we decorated the DPA with a carboxylate anchoring group that allows the dye to attach to the metal oxide surface while maintaining its photophysical properties. The dye (methyl 4-(10-*p*-tolylanthracen-9-yl)benzoate (MTAB)) was obtained from diiodoanthracene via two successive Suzuki coupling reactions with *p*-tolylboronic acid and (4-(methoxycarbonyl)phenyl)boronic acid. This rather simple modification gives several additional advantages over the DPA-based system. By chemically anchoring the emitter molecule we can minimize oxygen concentrations by embedding the system in a cell sealed under argon atmosphere inside a glovebox. This was not possible using physisorbed dyes since the heating applied for sealing of the cell caused desorption of the dyes from the surface. Additional advantages of the anchor group are that it allows for a higher dye loading and the use of a solvent more applicable for DSSCs. Using a solvent of lower polarity than water could improve the dye orientation on the surface of $ZrO_2$ and the orbital overlap between "emitters", which is necessary for efficient energy

**Chart 1. Heterogenous System for Photon Upconversion by Sensitized Triplet−Triplet Annihilation (UC-STTA)[a]**

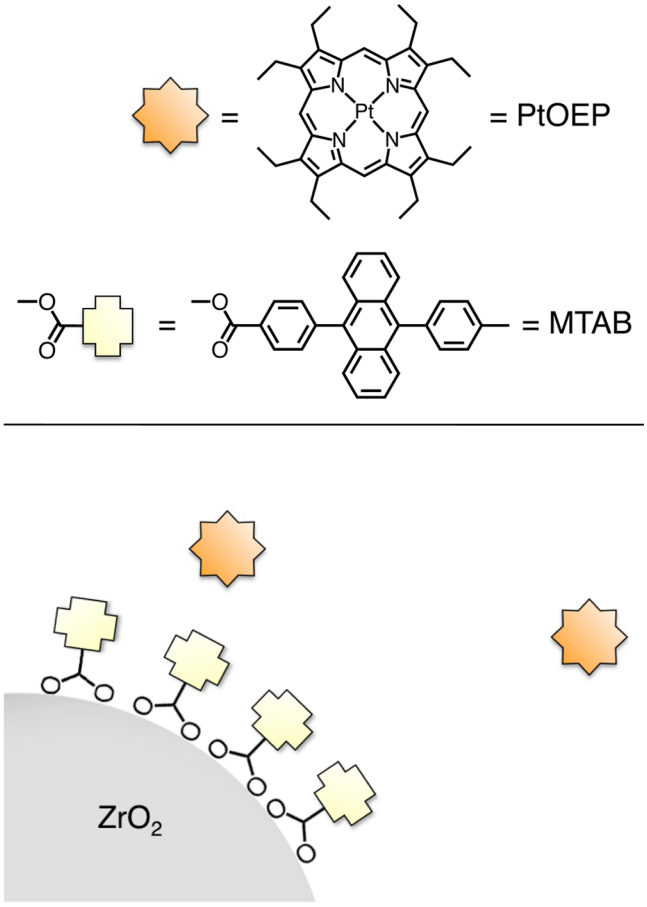


[a]Emitter molecules (MTAB) are chemisorbed onto mesoporous $ZrO_2$ thin film. Sensitizer molecules (PtOEP) are in a butyronitrile solution (BuN).

transfer. Butyronitrile (BuN) has been shown to have advantageous properties when used for electrolytes in DSSCs.[27] Choosing BuN as the solvent in the MTAB-based system allows us to have the PtOEP sensitizer molecules free in solution and thereby avoid potential energy traps from PtOEP aggregates formed on the $ZrO_2$ surface.

## EXPERIMENTAL SECTION

**Methyl 4-(10-*p*-Tolylanthracen-9-yl)benzoate (MTAB): Synthesis and Characterization.** In 30 mL of degassed dimethoxyethane was added 110 mg (0.25 mmol) of diiodoanthracene, 10 mol % (30 mg) [$Pd(PPh_3)_4$], and 70 mg (0.50 mmol) of *p*-tolylboronic acid. After addition of 70 mg (0.46 mmol) of CsF the mixture was heated to reflux for 2 h. After 2 h (4-(methoxycarbonyl)phenyl)boronic acid (77 mg 0.43 mmol) was added to the mixture and continued stirring for an additional 14 h. The mixture was then cooled to room temperature, and water was added. The water phase was washed with $CH_2Cl_2$, and the mixed organic phases were dried over $MgSO_4$. The solvent was removed under vacuum, and the crude product was purified by column chromatography (silica, $CH_2Cl_2$). The obtained yellow solid was further purified by column chromatography (silica, hexane:$CH_2Cl_2$ is 10:1) to obtain the pure product as a pale yellow solid (yield: 15%).

$^1$H NMR: $\delta$ = 8.29 (d, $J$ = 8.28 Hz, 2 H), 7.74 (dd, $J$ = 7.73, 7.74 Hz, 2 H), 7.63−7.56 (m, 4 H), 7.44−7.31 (m, 8 H), 4.02 (s, 3H), 2.55 (s, 3 H).

$^{13}$C NMR: $\delta$ = 167.27, 144.53, 138.01, 137.35, 135.89, 135.70, 131.70, 131.28, 130.09, 129.87, 129.69, 129.56, 129.39, 127.36, 126.59, 125.13, 121.20, 52.44, 21.56.

Elemental analysis calcd for $C_{29}H_{22}O_2$ + 2 × $C_6H_{14}$: C, 85.67; H, 8.77. Found: C, 84.59; H, 8.27. For more details see the Supporting Information.

**Samples.** The mesoporous $ZrO_2$ films were prepared on glass substrates either by screen printing (2.6 $\mu$m film thickness) or by a blade casting procedure described previously;[24] the thickness varied as indicated in the text. The films were sensitized by immersing them into a 1:3 volume:volume ratio of ethanol:acetonitrile (EtOH/AcN, Solveco/Merck, Uvasol) solution of either MTAB only (0.21−0.23 mM) or in a mixture with 10 mM deoxycholic acid (DCA) for 4−5 days. After the sensitization, the films were carefully rinsed by immersion for 1 day in 20 mL of AcN and for 1 day in 20 mL of BuN (Fluka). Our aim was to ensure that no loosely attached, physisorbed MTAB dyes remained in the sample. After such a rigorous rinsing procedure, the remaining dyes should be firmly anchored to the $ZrO_2$ surface.[28,30] The sensitized and rinsed films were finally built into a sealed cell by sandwiching the glass substrate with a cover glass (Menzel-Gläser) containing two holes for solvent injection. The two pieces of glass were separated by a frame of Surlyn (50 $\mu$m thickness, DuPont), which was subsequently melted using a soldering iron. The cells were transferred to a glovebox ($O_2$ < 0.1 ppm) where either neat BuN or a BuN solution with PtOEP ($5.5 \times 10^{-5}$−$7.6 \times 10^{-5}$ M, Aldrich) was injected. The cells were heat sealed using Surlyn and a microscope coverslip.

**Steady-State Spectroscopy.** Steady-state absorption and emission measurements were performed as stated previously.[24] Briefly, UV−vis absorption measurements were carried out using a Cary 5000 spectrophotometer (Varian). The spectra were analytically corrected for the scattering of the $ZrO_2$ films.

The steady-state emission spectra were recorded on a Fluorolog-3 fluorimeter (Horiba Jobin Yvon). A scattering correction for the emission spectra was not needed in the present study due to the much larger magnitude of the upconverted emission signal. Front-face illumination geometry (sample at 90° with respect to the incident beam) was used. For the upconversion measurements, the instrumental parameters were set as in ref 24 to allow for easy comparison of the UC intensities of the studied systems. To prevent second-order diffracted light from reaching the sample, a 380 nm long-pass filter was placed in front of the light source. In this setup the incident excitation intensity was 8 mW/cm$^2$ at 534 ± 5 nm. Details, as well as a description of the intensity dependence measurements, can be found in ref 24.

**Time-Resolved Emission Spectroscopy.** Time-resolved emission spectra were measured using 10 ns laser pulses at 10 Hz for excitation at 534 nm at an intensity of 3.9 mJ/cm$^2$ per pulse. The excitation light was directed through a Schott GG400 long-pass filter to avoid direct excitation of the MTAB dye due to residual 355 nm photons. The sample was placed approximately 30° with respect to the excitation beam. The emission spectra were recorded by a CCD camera in a direction perpendicular to the excitation light. To minimize scattered laser light different filters were placed in front of the CCD camera; a 550 nm long-pass filter was used to measure the


dx.doi.org/10.1021/jp402477q | J. Phys. Chem. C 2013, 117, 14493−14501

PtOEP phosphorescence, and a Schott BG12 filter was used to measure the UC emission. Both filters slightly distorted the recorded spectra. A detailed description of the experimental setup is available in ref 24.

**Time-Correlated Single-Photon Counting.** The samples were excited using a 404.6 nm picosecond diode laser (Edingburg Instruments, EPL-405) at a repetition rate of 5 MHz and with a pulse width of 77.1 ps. The excitation intensity was adjusted using a VBA-200 variable beam splitter (Jodon Engineering Associates) to yield a count rate of <1% of the excitation frequency. A cooled Hamamatsu MCP-photomultiplier R3809U-51 was used for the detection of single photons. The detected photons were polarized in "magic angle" (54.7°) with respect to the vertically polarized excitation light, and scattered laser light was blocked using a GG10 cutoff filter. For selection of red-edge MTAB fluorescence an additional set of optical filters (OG2 and VG9) was applied. Measurements were done in reverse mode using an instrumental setup described recently.[31] For each measurement a minimum of 15000 counts was collected in the channel of peak intensity. A glass slide (Menzel-Gläser) was used for recording the instrument response function (IRF) without the use of filters. The data were analyzed using the SpectraSolve program (Ames Photonics) applying an iterative reconvolution of the IRF with an exponential decay model with one, three, or four components.

## RESULTS AND DISCUSSION

**Characterization of Emitter and Sensitizer Dyes.** *Steady-State Electronic Spectra.* Figure 1 shows a comparison of the absorption and photoluminescence spectra of (a) MTAB and PtOEP in dilute solution (~$10^{-5}$ M) and (b) MTAB-sensitized $ZrO_2$ films (MTAB|$ZrO_2$) in BuN solution, with and without PtOEP. The sensitized $ZrO_2$ films were contained in sealed cells. No significant spectral changes are observed in the PtOEP absorption spectrum as the MTAB|$ZrO_2$ film is added to the system (compare Figures 1a and 1b). However, a careful inspection of the PtOEP phosphorescence spectra shows the appearance of a small shoulder around 760 nm. This same shoulder can be observed when MTAB is added to a BuN solution of PtOEP in sufficient concentration (see Figure S2 in Supporting Information) and can therefore be ascribed to some sort of ground- or excited-state complexation between PtOEP and MTAB. The small magnitude of this feature suggests that PtOEP aggregate formation is effectively limited in this system compared to the previously studied system where PtOEP was intentionally adsorbed onto the $ZrO_2$ nanostructure.[24] In the prior system, a broad photoluminescence band with maximum intensity around 780 nm was attributed to PtOEP dimer phosphorescence.

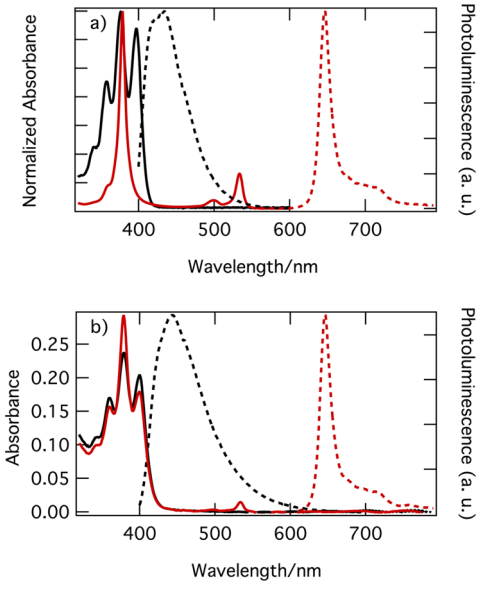


**Figure 1.** (a) Steady-state absorption (solid lines) and corrected photoluminescence (dashed lines) spectra of MTAB (black, $\lambda_{exc}$ = 393 nm) and PtOEP (red, $\lambda_{exc}$ = 534 nm) in dilute butyronitrile (BuN) solution. (b) Steady-state absorption (solid lines) and corrected photoluminescence (dashed lines) spectra of MTAB- ($\lambda_{exc}$ = 393 nm) sensitized $ZrO_2$ nanocrystalline films in BuN, without (black) and with (red) PtOEP ($\lambda_{exc}$ = 534 nm) in solution. The thickness of the films was 2.6 $\mu$m. The absorption spectra measured on films have been analytically corrected for the scattering of the samples (see ESI of ref 24).

The absorption spectrum of the MTAB dye appears to be relatively unaffected by the anchoring onto the $ZrO_2$ surface (compare Figures 1a and 1b). The only change observed is a 2−3 nm bathochromic shift upon chemisorption of the dye. This comparison indicates that no significant amount of ground-state aggregation takes place between MTAB molecules on the $ZrO_2$ surface.

A difference in the steady-state fluorescence spectra was observed for the comparison of MTAB in solution and on $ZrO_2$ (see Figure 2); the fluorescence spectrum of adsorbed MTAB (red trace) clearly shows a loss of vibrational structure and a shift of the maximum to the red compared to MTAB in solution (black dashed trace). The magnitude of the shift and the loss of the vibrational structure depend on the concentration of MTAB in the sensitization solution and sensitization/rinsing times, i.e., surface coverage, as well as film thickness (see Figure S3 in the Supporting Information). The addition of deoxycholic acid (DCA) to the sensitization solution increases the vibrational structure and minimizes the red shift of the fluorescence spectrum of MTAB adsorbed onto $ZrO_2$ (Figure 2, black solid vs red solid traces).

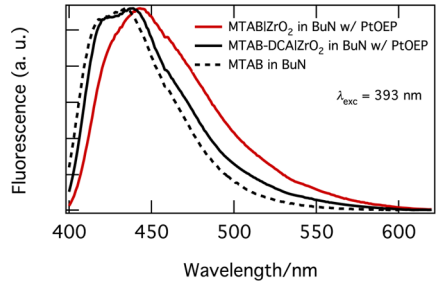


**Figure 2.** Effect on the MTAB|$ZrO_2$ fluorescence spectrum of adding the coadsorbent deoxycholic acid (DCA) to the sensitization solution (10 mM). The thickness of both $ZrO_2$ films was 2.6 $\mu$m. The fluorescence spectrum of MTAB in BuN solution is shown for comparison (dashed line).

*Time-Resolved Fluorescence.* The fluorescence lifetime of MTAB free in solution and bound to $ZrO_2$ was determined by TCSPC. In dilute AcN solution (~$10^{-5}$ M) the MTAB fluorescence decays exponentially with a lifetime of 4.3 ns (see Figure S5 in Supporting Information).


dx.doi.org/10.1021/jp402477q | J. Phys. Chem. C 2013, 117, 14493−14501

For MTAB adsorbed onto $ZrO_2$ the fluorescence decay is nonexponential with an observed average lifetime of 1.6 ns (see Figure S6 in Supporting Information). Moreover, it was observed that the average fluorescence lifetime of MTAB on $ZrO_2$ increases as the monitored fluorescence wavelength increases. This observation can be explained by homogeneous radiative energy transfer (inner-filter effect) among the MTAB dyes, which are highly concentrated within the $ZrO_2$ nanostructure, and by the use of front-face detection geometry.[32] Homogeneous radiative energy transfer could also explain the spectral shape of the MTAB fluorescence discussed above and illustrated in Figure 2 and Figure S3 (Supporting Information). It should be noted, though, that a similar effect on the fluorescence lifetime and spectral shape could be expected from excimer formation.[33]

*Adsorption/Desorption of MTAB Molecules.* MTAB is soluble in BuN. Even though the majority of the emitter dye molecules is covalently bound to the $ZrO_2$ surface, an equilibrium will be established between the surface and liquid phases. From this we believe that some small fraction of emitter dyes will be present in the bulk solution. Since those molecules could potentially play a role in the upconversion mechanism, we decided to measure the concentration of emitter dyes in the bulk solution.

With this aim, a $ZrO_2$ film (3.4 $\mu$m thickness) was sensitized and rinsed according to the procedure described in the Experimental Section and subsequently left in 500 $\mu$L of BuN solution for 1.5 h. This time interval is the maximum time passing between cell sealing and emission measurements in our experimental procedures. Hereafter, 400 $\mu$L of the BuN solution was transferred to a 2 mm cuvette. The concentration of desorbed MTAB molecules in this volume was too low to be quantified in an absorption measurement and was therefore measured by fluorimetry. A calibration series, relating fluorescence signal to absorbance, was thereafter made, and the fluorescence intensity measured on the desorbed MTAB molecules could be ascribed to a certain concentration (see Supporting Information for details). From this we calculated that the maximum MTAB concentration desorbed into bulk solution for the sealed cells was 1.3 $\mu$M.

**Photon Upconverted Emission.** Excitation in the PtOEP Q-band (534 nm) of the sealed cells containing MTAB sensitized nanostructured $ZrO_2$ films gives rise to an anti-Stokes emission signal that matches well with the singlet emission from MTAB and with an intensity maximum around 430 nm (see Figure 3). A similar cell was prepared in the absence of PtOEP and excited at 534 nm, which produced no anti-Stokes emission. We, therefore, attribute the anti-Stokes emission seen in the PtOEP-containing system to UC-STTA mediated by triplet energy transfer from PtOEP to MTAB. It is noteworthy that the UC emission spectrum is blue-shifted with respect to the prompt fluorescence spectrum (compare solid and dashed red traces in Figure 3, inset).

As expected, the absolute magnitude of the observed UC signal of the MTAB|$ZrO_2$ sealed cell system is significantly enhanced when compared with the previously studied DPA-based system (compare solid red and green traces in Figure 3). The enhancement to the upconverted emission signal may be attributed to several factors. First, the orientation of the emitter molecule on the surface of $ZrO_2$ may be drastically different from the previous study, due to the presence of an anchoring group and the use of a less polar solvent. Instead of lying flat on the surface of $ZrO_2$, MTAB can stand on the surface and have

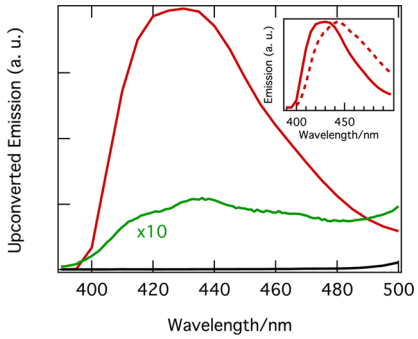


**Figure 3.** Comparison of the relative intensity for (red, solid) steady-state upconverted emission of MTAB|$ZrO_2$ in a sealed cell containing a BuN solution of PtOEP ([PtOEP] = 5.5 × $10^{-5}$ M, $\lambda_{exc}$ = 534 nm, incident power density = 8 mW/cm$^2$) and (green) the UC signal measured in a previously studied DPA–PtOEP|$ZrO_2$ cosensitized system (film thickness is 5.3 $\mu$m).[24] (Black) Emission spectrum ($\lambda_{exc}$ = 534 nm) of MTAB|$ZrO_2$ in BuN (no PtOEP) measured under conditions similar to those used for the sample containing PtOEP. (Inset, red, dashed) Fluorescence spectrum ($\lambda_{exc}$ = 393 nm) of the MTAB|$ZrO_2$ sample containing PtOEP (normalized to the magnitude of the upconverted signal).

improved overlap between the $\pi$ orbitals of adjacent MTAB dyes. This will enhance triplet energy migration among the emitter dyes. Second, preparation of sealed samples under Ar atmosphere decreases dramatically the amount of oxygen in the sample, removing the main quenching mechanism of the triplet states of both PtOEP and MTAB, as well as improving the stability of the sample by suppressing endoperoxide formation in the emitter dye.[34] Finally, the use of a less polar solvent inhibits the formation of porphyrin dimers, removing an additional quenching path of PtOEP triplets.

It should be noted that the data shown here are all measured on $ZrO_2$ films with nonoptimized surface coverage. The surface coverage is low due to the rigorous rinsing procedure applied, which causes desorption and removal of loosely or weakly adsorbed MTAB dyes. This will affect the triplet energy transfer from PtOEP to MTAB and will limit the excitation migration across the nanoparticle surface. While the rinsing procedure decreases upconversion efficiency for our samples, it allows for a controlled, well-defined system that is more suitable to the fundamental purposes of our work. A rough estimate of the surface coverage was calculated to be ∼10% of a monolayer following procedures and assumptions of Gardner et al.[35] At this coverage, assuming a homogeneous distribution of molecules, we calculate a distance of ∼2 nm between MTAB molecules on the surface of $ZrO_2$. For data from ref 24, a similar distance of ∼2 nm was calculated for the distance between DPA molecules on the surface of $ZrO_2$. Since chemisorbed MTAB molecules are expected to occupy less surface area than physisorbed DPA molecules, dye loading will be higher in the case of MTAB (∼75 molecules per nanoparticle vs ∼42 molecules per nanoparticle in the case of DPA). As mentioned before, improved performance for MTAB-sensitized $ZrO_2$ may be due to improved orbital overlap between adjacent MTAB molecules and decreased oxygen levels in the sealed cells.

*Bound vs Free MTAB.* Sealed cells were produced containing 5.5 × $10^{-5}$ M PtOEP and varying MTAB concentrations in homogeneous BuN solution. The samples were prepared under Ar atmosphere, in identical conditions as described above, but in this case, due to the absence of $ZrO_2$, both emitter and


dx.doi.org/10.1021/jp402477q | J. Phys. Chem. C 2013, 117, 14493−14501

sensitizer dyes were free to diffuse in solution. Even though the highest MTAB concentration studied ($2.1 \times 10^{-4}$ M) was similar to the concentration used in the sensitization of the $ZrO_2$ films (see Experimental Section), none of these only liquid samples produced an UC signal on the order of magnitude observed in the MTAB|$ZrO_2$ system (see Figure 4).

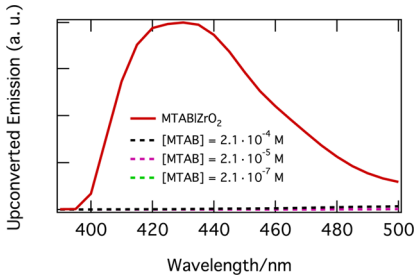


**Figure 4.** Steady-state upconverted emission spectrum ($\lambda_{exc}$ = 534 nm) of a sealed cell containing MTAB|$ZrO_2$ in a BuN solution of PtOEP ($5.5 \times 10^{-5}$ M), red trace. The dashed traces represent the UC signals measured under similar conditions for three sealed cells containing BuN solutions of MTAB in various concentrations (see color code in graph) and PtOEP ($5.5 \times 10^{-5}$ M for all cells).

In principle, this was a surprising result since upconversion in solution is usually much more efficient than in the solid state, a fact attributed to the low mobility of the involved chromophores in the solid medium.[8] However, it should be considered that adsorption of the emitter onto $ZrO_2$ enhances the local concentration of energy acceptors, which should favor triplet energy migration and TTA.

Regardless of the reason for the low efficiency in solution, Figure 4 shows that the majority of the observed UC emission in the heterogeneous sample (MTAB|$ZrO_2$ in a BuN solution of PtOEP) must originate from the bound, adsorbed emitters and cannot be attributed to the small fraction of free MTAB in solution (1.3 $\mu$M). Estimates of the UC-STTA quantum yields for the studied systems are shown in Table 1 (see Supporting Information for details).

**Table 1. Estimated UC-STTA Quantum Yields, $\Phi_{UC}$, for the Studied Systems**

| system[a] | $\Phi_{UC}$ [%] |
|---|---|
| MTAB|$ZrO_2$ in a BuN solution of PtOEP ($5.5 \times 10^{-5}$ M)[b,c] | ~0.04 |
| MTAB ($2.1 \times 10^{-4}$ M) and PtOEP ($5.5 \times 10^{-5}$ M) in a BuN solution[c] | ~$5 \times 10^{-4}$ |
| DPA-PtOEP|$ZrO_2$ in water[d] | ~$6 \times 10^{-4}$ |

[a]Experimental conditions: samples excited at 534 (MTAB as emitter dye) or 536 nm (DPA as emitter dye), 10 nm bandpass, with a power density of 8 mW/cm$^2$ at room temperature and under anaerobic conditions. [b]Value calculated for the system presented in Figures 1b and 3. [c]Estimated using $Ru(bpy)_3Cl_2$ in air-equilibrated water as a standard quantum yield. [d]From ref 24. Estimated using the sample's prompt fluorescence as the internal reference.

**Photon Upconversion Dependence on Incident Light Intensity.** The magnitude of the photon upconversion signal was monitored at different incident light intensities, ranging from 0.5 to 7.6 mW/cm$^2$. The range of excitation intensities was determined by the Xe-lamp intensity (upper limit) and the appearance of upconversion emission (lower limit). Figure 5 shows the integrated upconverted emission (red crosses) vs excitation power density on MTAB|$ZrO_2$ in a sealed cell

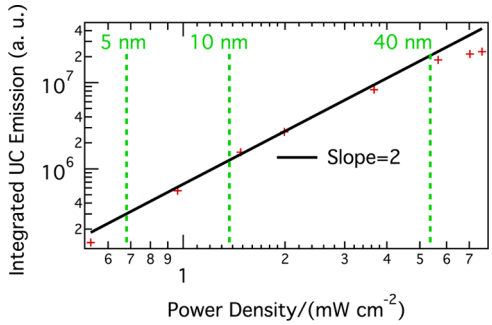


**Figure 5.** Integrated upconverted emission (red crosses) vs excitation power density in MTAB|$ZrO_2$ in a sealed cell containing a BuN solution of PtOEP ([PtOEP] = $5.5 \times 10^{-5}$ M, $\lambda_{exc}$ = 534 nm) and quadratic power dependence fit (black solid line). The green vertical dashed lines indicate the power density supplied by the sun at 534 nm under AM 1.5 conditions integrated over 5 nm (534 ± 2.5 nm), 10 nm (534 ± 5 nm), and 40 nm (534 ± 20 nm), respectively. While the upconverted emission shows a quadratic dependence on incident power at very low excitation intensities, it approaches linear behavior at higher excitation intensities. This is a sign that the system is reaching the so-called "strong annihilation limit", further explained in the main body.

containing a BuN solution of PtOEP ([PtOEP] = $5.5 \times 10^{-5}$ M, $\lambda_{exc}$ = 534 nm) and quadratic power dependence fit (black solid line). The green vertical dashed lines indicate the power density supplied by the sun under AM 1.5 conditions at 534 nm, maximum of PtOEP Q-band, integrated over 534 ± 2.5, 534 ± 5, and 534 ± 20 nm, respectively. The studied range corresponds to excitation power densities comparable to what would be obtained by sunlight irradiation.

The upconverted emission shows a quadratic dependence on incident power at very low excitation intensities. Such nonlinear dependence is expected in TTA processes[36] and is often used as a proof of their presence.[13,37] Similar behavior has previously been observed in UC-STTA studies at similar excitation intensities of other solid-state systems such as rubbery polymer blends[38] and rigid polymer films,[39] among others.[40,41] Of greater interest is the fact that the dependence approaches a linear regime at higher excitation intensities. Such behavior is predicted to occur in systems where the main deactivation path of the triplet is TTA[42,43] and implies a highly efficient TTA process. While the so-called "strong annihilation limit" is usually reached at very high excitation intensities using laser emission as the excitation source, it has recently been shown that this regime can also be reached with sunlight-like excitation intensities if the system is thoroughly deoxygenated, that is, if the most common triplet quenching mechanism is eliminated.[16,44] Our results agree well with these previous reports and indicate that, in spite of the nonoptimal surface coverage, efficient TTA can be reached on MTAB-sensitized $ZrO_2$.

**Time-Resolved UC Emission Measurements.** Figure 6 shows the time-resolved Stokes and anti-Stokes emissions, respectively, PtOEP phosphorescence and MTAB upconverted emission, resulting from 534 nm excitation of a sealed cell containing MTAB|$ZrO_2$ and PtOEP in BuN solution. Due to the low amplitude of the signal a rather long time window (500 ns) was needed for integration of each spectrum; therefore, the number of data points is too few to allow for a proper modeling of the dynamics. In spite of this, some important qualitative information is available from the data. It is clear that the main part of the UC-STTA signal (anti-Stokes emission) shows a


dx.doi.org/10.1021/jp402477q | J. Phys. Chem. C 2013, 117, 14493−14501

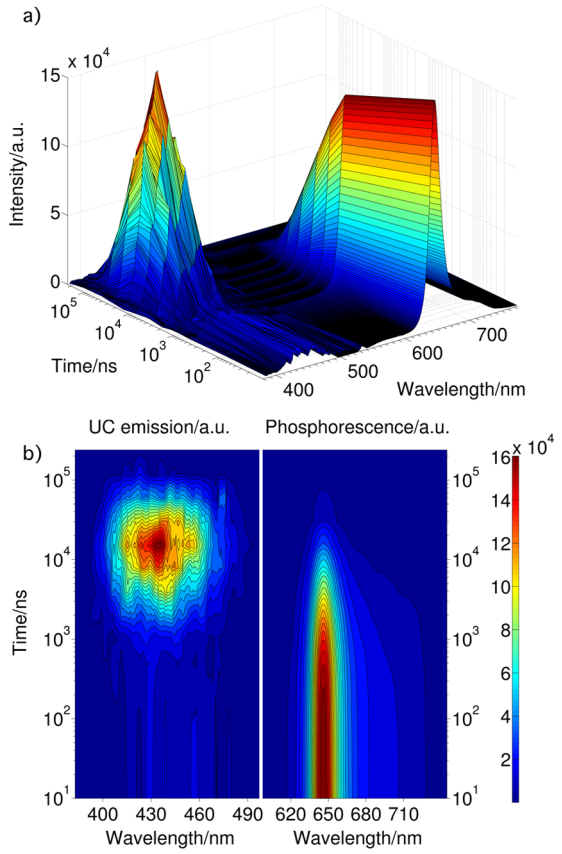


**Figure 6.** (a) Time-resolved UC emission (anti-Stokes emission) and PtOEP phosphorescence decay (Stokes emission) of a sealed cell containing MTAB|$ZrO_2$ and PtOEP ($7.6 \times 10^{-5}$ M) in BuN.[48] The $ZrO_2$ film thickness is 2.2 $\mu$m. Excitation wavelength is 534 nm. (b) A contour representation of the data in (a).

very slow rise time, with the maximum amplitude reached 15 $\mu$s after the excitation pulse. This result is in contrast to the previously studied DPA−PtOEP cosensitized $ZrO_2$ films, where the anti-Stokes signal showed a rise time ≤10 ns.[24] In that system the PtOEP molecules were adsorbed onto the $ZrO_2$ along with the DPA, which allowed for "static" energy migration and TTA. In the present case of MTAB|$ZrO_2$, the sensitizer (PtOEP) is in solution and in low concentration ($7.1 \times 10^{-5}$ M) to avoid the formation of aggregates. Due to this condition, PtOEP molecules are required to diffuse to the MTAB|$ZrO_2$ surface for the initial energy transfer step to take place, which explains the slow rise of the UC signal. The decay of the UC signal is slow and does not follow a power law (for more details, see Figure S8 and accompanying text in the Supporting Information). Upconverted photons are still detected after 100 $\mu$s.

The decay of the PtOEP phosphorescence (Stokes emission) is nonexponential (see Figure 6 and Figure S8 in the Supporting Information). Most of the phosphorescence decay occurs on a microsecond time scale, mirroring the slow rise of the UC emission. Only a small fraction of excited PtOEP is deactivated by TET to the surface-bound MTAB. The poor sensitization efficiency can be explained if we consider the diffusion of the PtOEP molecules in the studied system. The monitored sealed samples have an inner thickness of 50 $\mu$m, where only about 3 $\mu$m is due to the mesoporous $ZrO_2$; bulk PtOEP in BuN solution comprises most of the sample. Consequently, the majority of the excited PtOEP molecules in the bulk solution will never reach the $ZrO_2$ surface (the diffusion length of excited PtOEP is about 300 nm in deoxygenated solvents[45]). TET inside the nanostructured film should be more efficient because of the proximity of the porphyrins to the MTAB molecules chemisorbed to the $ZrO_2$ surface; pore diameters are typically in the order of a few nanometers.[29,46] However, due to the low PtOEP concentration in solution and the small volumes involved, only a minuscule fraction of the excited PtOEP sensitizers will be inside the film pores. Moreover, the sensitizer diffusion through the pore network will be greatly reduced with respect to that of bulk.[29,30,46] Consequently, TET occurring inside the nanostructured film pores should not significantly affect the overall phosphorescence decay rate.

The fact that the energy transfer from excited PtOEP to MTAB is not efficient will have important consequences for the studied upconverting system. First, the overall efficiency of the UC-STTA process will be significantly limited. We estimate a UC quantum yield of ∼0.04% for the studied system under 8 mW/cm$^{-2}$ excitation intensity. UC efficiencies of ∼10% have been reported for a soft host matrix doped with DPA and PtOEP under similar excitation conditions.[14] Second, the concentration of MTAB triplets will be low and most probably not homogeneous in the $ZrO_2$ film. Considering that the amount of excited PtOEP *inside* the pores will be very low and that the amount of excited PtOEP diffusing from the bulk *into* the film should be negligible (most of the incoming excited sensitizers will be quenched at the interface; diffusion inside the nanostructure will be slow), it is to be expected that the highest concentration of MTAB triplets will occur at the interface between the film and the bulk. This inhomogeneous distribution of the MTAB triplets will affect the TTA efficiency. Since TTA, and therefore the UC process, will be more efficient where the concentration of triplet MTAB is higher, it could be expected that upconversion will be more efficient at the interface between the film and the bulk solution. This hypothesis agrees well with the steady-state fluorescence measurements reported above (see Figure 3, inset). The UC emission spectrum is blue-shifted with respect to the prompt fluorescence spectrum, as it would be expected if UC mainly occurred at the interface between film and bulk solution, minimizing the reabsorption of the emitted photons (inner-filter effect).

The PtOEP phosphorescence decay also presents a small, but fast, component (<20 ns), along with the decay of a PtOEP hot emission band (see Figure S9 in the Supporting Information).[47] A plausible reason for this short decay component would be that a minor fraction of PtOEP is physisorbed onto $ZrO_2$. This could also explain the small part of the UC (anti-Stokes) emission that shows "static" behavior, i.e., rise time ≤ 10 ns (see Figure 6).

Taken as a whole, the time-resolved data support a mechanism where homogeneous TTA (between two MTAB triplets) is involved to some extent. This is due to the observation that UC photons are detected after the PtOEP phosphorescence is gone. From our present data, we choose not to speculate whether heterogeneous TTA (between MTAB and PtOEP triplets) contributes to the UC signal at shorter time scales. We plan to carry out more detailed time-resolved studies to get a more complete picture of the mechanistic details of the system.


dx.doi.org/10.1021/jp402477q | J. Phys. Chem. C 2013, 117, 14493−14501

## SUMMARY

Using sunlight-like conditions we have shown a dramatic increase in photon upconversion efficiency on a surface. The estimated UC quantum yield showed a 60-fold increase relative to a similar system based on 9,10-diphenylanthracene (DPA) previously reported.[24] The introduction of an anchoring group onto the emitter molecule increased dye loading and allowed us to use a sensitizer in solution, inhibiting its aggregation. The degradation pathways observed in previous studies were obviated in the present system by the use of cells sealed in a glovebox.

The new system approaches a linear dependence of upconverted emission magnitude on excitation intensity. A linear regime implies that the "strong annihilation limit" has been reached. At this limit the main deactivation pathway for MTAB triplets is triplet−triplet annihilation, which implies that the former mechanism is *not* the rate-limiting step in the upconversion process. It is conceivable that the anchoring group introduced in MTAB causes an increased orbital overlap between adjacent MTAB molecules contributing positively to the high efficiency of triplet−triplet annhilation observed in this system. It is remarkable that the system gets close to the "strong annihilation limit" at light intensities which are provided by the sun without concentration of the light. Time-resolved data suggest that sensitization via dynamic triplet energy transfer must be the largest factor limiting upconversion efficiency.

Transient emission data showed a slow rise of the upconverted signal with the maximum amplitude reached 15 $\mu$s after the excitation pulse, which suggests that diffusion of PtOEP triplet excited states to MTAB molecules on the $ZrO_2$ surface is the limiting step for UC-STTA in this system. One important consequence of the limiting diffusion step is that the UC-STTA process is only efficient at the interface between the nanostructure and the bulk solution. For further improvement of the UC-STTA efficiency on mesoporous metal oxides, we therefore propose the introduction of an anchoring group on the porphyrin sensitizer molecule. This would allow for highly efficient triplet energy transfer between sensitizer and emitter molecules and thereby increase the overall efficiency of UC-STTA on nanostructured metal oxides, taking a step further toward application of this upconversion strategy in DSSCs.

## ASSOCIATED CONTENT

### Supporting Information

MTAB synthesis, sample description, PtOEP−MTAB aggregate photoluminescence, MTAB|$ZrO_2$ 1 $\mu$m thin film absorption and fluorescence spectra, TCSPC data for MTAB fluorescence decay in solution and on $ZrO_2$, MTAB absorbance−fluorescence calibration series, additional time-resolved UC emission analysis, PtOEP photoluminescence decay on a short time scale, and UC quantum yield evaluation and method. This material is available free of charge via the Internet at http://pubs.acs.org.

## AUTHOR INFORMATION

### Corresponding Author

*E-mail: ana.morandeira@kemi.uu.se.

### Notes

The authors declare no competing financial interest.

## ACKNOWLEDGMENTS

We thank L. Häggman (Uppsala University, Sweden) for his help in the preparation of the $ZrO_2$ paste and Mohammad Mirmohades (Uppsala University, Sweden) for his help with the time-resolved UC emission measurements. JG thanks the Swedish Government's Strategic Research Area: STandUP for ENERGY. JL thanks the C F Liljewalchs Foundation for a travel scholarship. This work was supported by the Swedish Research Council (VR), the Knut and Alice Wallenberg Foundation, Gran Gustafsson Foundation, and the Swedish Energy Agency.

## REFERENCES

(1) Rullière, C., Ed. *Femtosecond Laser Pulses*; Springer-Verlag: Berlin Heidelberg, 1998.
(2) Shockley, W.; Queisser, H. J. *J. Appl. Phys.* **1961**, *32*, 510.
(3) de Wild, J.; Meijerink, A.; Rath, J. K.; van Sark, W. G. J. H. M.; Schropp, R. E. I. *Energy Environ. Sci.* **2011**, *4*, 4835−4848.
(4) Huang, X.; Han, S.; Huang, W.; Liu, X. *Chem. Soc. Rev.* **2013**, *42*, 173−201.
(5) Zou, W.; Visser, C.; Maduro, J. A.; Pshenichnikov, M. S.; Hummelen, J. C. *Nat. Photonics* **2012**, *6*, 560−564.
(6) Baluschev, S.; Yakutkin, V.; Miteva, T.; Avlasevich, Y.; Chernov, S.; Aleshchenkov, S.; Nelles, G.; Cheprakov, A.; Yasuda, A.; Mullen, K.; Wegner, G. *Angew. Chem., Int. Ed.* **2007**, *46*, 7693−7696.
(7) Cates, E. L.; Chinnapongse, S. L.; Kim, J.-H.; Kim, J.-H. *Environ. Sci. Technol.* **2012**, *46*, 12316−12328.
(8) Singh-Rachford, T. N.; Castellano, F. N. *Coord. Chem. Rev.* **2010**, *254*, 2560−2573.
(9) Zhao, J.; Ji, S.; Guo, H. *RSC Adv.* **2011**, *1*, 937−950.
(10) Monguzzi, A.; Tubino, R.; Hoseinkhani, S.; Campione, M.; Meinardi, F. *Phys. Chem. Chem. Phys.* **2012**, *14*, 4322−4332.
(11) Simon, Y. C.; Weder, C. *J. Mater. Chem.* **2012**, *22*, 20817−20830.
(12) Keivanidis, P. E.; Baluschev, S.; Miteva, T.; Nelles, G.; Scherf, U.; Yasuda, A.; Wegner, G. *Adv. Mater. (Weinheim, Ger.)* **2003**, *15*, 2095.
(13) Kozlov, D. V.; Castellano, F. N. *Chem. Commun.* **2004**, 2860−2861.
(14) Monguzzi, A.; Bianchi, F.; Bianchi, A.; Mauri, M.; Simonutti, R.; Ruffo, R.; Tubino, R.; Meinardi, F. *Adv. Energy Mater.* **2013**, *3*, 680−686.
(15) Simon, Y. C.; Bai, S.; Sing, M. K.; Dietsch, H.; Achermann, M.; Weder, C. *Macromol. Rapid Commun.* **2012**, *33*, 498−502.
(16) Kim, J.-H.; Deng, F.; Castellano, F. N.; Kim, J.-H. *Chem. Mater.* **2012**, *24*, 2250−2252.
(17) Cheng, Y. Y.; Fückel, B.; MacQueen, R. W.; Khoury, T.; Clady, R. G. C. R.; Schulze, T. F.; Ekins-Daukes, N. J.; Crossley, M. J.; Stannowski, B.; Lips, K.; Schmidt, T. W. *Energy Environ. Sci.* **2012**, *5*, 6953−6959.
(18) Schulze, T. F.; Czolk, J.; Cheng, Y.-Y.; Fückel, B.; MacQueen, R. W.; Khoury, T.; Crossley, M. J.; Stannowski, B.; Lips, K.; Lemmer, U.; Colsmann, A.; Schmidt, T. W. *J. Phys. Chem. C* **2012**, *116*, 22794−22801.
(19) Khnayzer, R. S.; Blumhoff, J.; Harrington, J. A.; Haefele, A.; Deng, F.; Castellano, F. N. *Chem. Commun.* **2012**, *48*, 209−211.
(20) Kim, J.-H.; Kim, J.-H. *J. Am. Chem. Soc.* **2012**, *134*, 17478−17481.
(21) Kang, J.-H.; Reichmanis, E. *Angew. Chem.* **2012**, *124*, 12011−12014.
(22) Liu, Q.; Yin, B.; Yang, T.; Yang, Y.; Shen, Z.; Yao, P.; Li, F. *J. Am. Chem. Soc.* **2013**, *135*, 5029−5037.
(23) Ekins-Daukes, N. J.; Schmidt, T. W. *Appl. Phys. Lett.* **2008**, *93*, 063507.
(24) Lissau, J. S.; Gardner, J. M.; Morandeira, A. *J. Phys. Chem. C* **2011**, *115*, 23226−23232.

(25) Giaimuccio, J. M.; Rowley, J. G.; Meyer, G. J.; Wang, D.; Galoppini, E. *Chem. Phys.* **2007**, *339*, 146−153.
(26) Kay, A.; Humphry-Baker, R.; Graetzel, M. *J. Phys. Chem.* **1994**, *98*, 952−959.
(27) Sauvage, F.; Chhor, S.; Marchioro, A.; Moser, J.-E.; Graetzel, M. *J. Am. Chem. Soc.* **2011**, *133*, 13103−13109.
(28) O'Regan, B.; Xiaoe, L.; Ghaddar, T. *Energy Environ. Sci.* **2012**, *5*, 7203−7215.
(29) Dürr, M.; Schmid, A.; Obermaier, M.; Yasuda, A.; Nelles, G. *J. Phys. Chem. A* **2005**, *109*, 3967−3970.
(30) Dürr, M.; Obermaier, M.; Yasuda, A.; Nelles, G. *Chem. Phys. Lett.* **2009**, *467*, 358−360.
(31) El-Zohry, A.; Orthaber, A.; Zietz, B. *J. Phys. Chem. C* **2012**, *116*, 26144−26153.
(32) Pereira, E. J. N.; Berberan-Santos, M. N.; Fedorov, A.; Vincent, M.; Gallay, J.; Martinho, J. M. G. *J. Chem. Phys.* **1999**, *110*, 1600−1610.
(33) DPA does not form an excimer in solution (steric reasons). However, it has been observed for other anthracene derivatives that excimer formation is enhanced at high surface coverages on sensitized mesoporous $ZrO_2$.[25]
(34) Bouas-Laurent, H.; Castellan, A.; Desvergne, J.-P.; Lapouyade, R. *Chem. Soc. Rev.* **2000**, *29*, 43−55.
(35) Gardner, J. M.; Beyler, M.; Karnahl, M.; Tschierlei, S.; Ott, S.; Hammarström, L. *J. Am. Chem. Soc.* **2012**, *134*, 19322−19325.
(36) Parker, C. A. *Photoluminescence of Solutions*; Elsevier Publishing Company: Amsterdam, 1968.
(37) (a) Islangulov, R. R.; Kozlov, D. V.; Castellano, F. N. *Chem. Commun.* **2005**, 3776−3778. (b) Zhao, W.; Castellano, F. N. *J. Phys. Chem. A* **2006**, *110*, 11440−11445.
(38) (a) Islangulov, R. R.; Lott, J.; Weder, C.; Castellano, F. N. *J. Am. Chem. Soc.* **2007**, *129*, 12652−12653. (b) Singh-Rachford, T. N.; Lott, J.; Weder, C.; Castellano, F. N. *J. Am. Chem. Soc.* **2009**, *131*, 12007−12014.
(39) Merkel, P. B.; Dinnocenzo, J. P. *J. Lumin.* **2009**, *129*, 303−306.
(40) Monguzzi, A.; Tubino, R.; Meinardi, F. *J. Phys. Chem. A* **2009**, *113*, 1171−1174.
(41) Monguzzi, A.; Frigoli, M.; Larpent, C.; Tubino, R.; Meinardi, F. *Adv. Funct. Mater.* **2012**, *22*, 139−143.
(42) Monguzzi, A.; Mezyk, J.; Scotognella, F.; Tubino, R.; Meinardi, F. *Phys. Rev. B* **2008**, *78*, 195112.
(43) Auckett, J. E.; Chen, Y. Y.; Khoury, T.; Clady, R. G. C. R.; Ekins-Daukes, N. J.; Crossley, M. J.; Schmidt, T. W. *J. Phys: Conf. Ser.* **2009**, *185*, 012002 (4pp).
(44) Haefele, A.; Blumhoff, J.; Khnayzer, R. S.; Castellano, F. N. *J. Phys. Chem. Lett.* **2012**, *3*, 299−303.
(45) Bansal, A.; Holzer, W.; Penzkofer, A.; Tsuboi, T. *Chem. Phys.* **2006**, *330*, 118−129.
(46) Vargas-Florencia, D.; Edvinsson, T.; Hagfeldt, A.; Furó, I. *J. Phys. Chem. C* **2007**, *111*, 7605−7611.
(47) Kalinowski, J.; Stampor, W.; Szmytkowski, J.; Cocchi, M.; Virgili, D.; Fattori, V.; Di Marco, P. *J. Chem. Phys.* **2005**, *122*, 154710.
(48) The sampling width of each spectrum was 500 ns, and the bandpass of the monochromator was 5 nm. Between 30 and 100 measurements were made and averaged for each spectrum. The data have been normalized, so the maxima of both signals are the same. The spectra were smoothed using a built-in MATLAB procedure.